

## Measurement of the near-threshold $e^+e^- \rightarrow D\bar{D}$ cross section using initial-state radiation

G. Pakhlova,<sup>14</sup> I. Adachi,<sup>9</sup> H. Aihara,<sup>42</sup> K. Arinstein,<sup>1</sup> V. Aulchenko,<sup>1</sup> T. Aushev,<sup>14,18</sup> A. M. Bakich,<sup>39</sup> V. Balagura,<sup>14</sup> A. Bay,<sup>18</sup> I. Bedny,<sup>1</sup> U. Bitenc,<sup>15</sup> A. Bondar,<sup>1</sup> A. Bozek,<sup>27</sup> M. Bračko,<sup>15,20</sup> J. Brodzicka,<sup>9</sup> T. E. Browder,<sup>8</sup> P. Chang,<sup>26</sup> A. Chen,<sup>24</sup> W. T. Chen,<sup>24</sup> B. G. Cheon,<sup>7</sup> R. Chistov,<sup>14</sup> S.-K. Choi,<sup>6</sup> Y. Choi,<sup>38</sup> J. Dalseno,<sup>21</sup> M. Danilov,<sup>14</sup> A. Drutskoy,<sup>3</sup> S. Eidelman,<sup>1</sup> D. Epifanov,<sup>1</sup> N. Gabyshev,<sup>1</sup> B. Golob,<sup>15,19</sup> K. Hayasaka,<sup>22</sup> H. Hayashii,<sup>23</sup> D. Heffernan,<sup>32</sup> Y. Hoshi,<sup>41</sup> W.-S. Hou,<sup>26</sup> H. J. Hyun,<sup>17</sup> T. Iijima,<sup>22</sup> K. Inami,<sup>22</sup> A. Ishikawa,<sup>35</sup> H. Ishino,<sup>43</sup> R. Itoh,<sup>9</sup> Y. Iwasaki,<sup>9</sup> D. H. Kah,<sup>17</sup> J. H. Kang,<sup>47</sup> N. Katayama,<sup>9</sup> H. Kawai,<sup>2</sup> T. Kawasaki,<sup>29</sup> A. Kibayashi,<sup>9</sup> H. Kichimi,<sup>9</sup> H. O. Kim,<sup>17</sup> S. K. Kim,<sup>37</sup> Y. J. Kim,<sup>5</sup> K. Kinoshita,<sup>3</sup> S. Korpar,<sup>15,20</sup> P. Krokovny,<sup>9</sup> R. Kumar,<sup>33</sup> C. C. Kuo,<sup>24</sup> A. Kuzmin,<sup>1</sup> Y.-J. Kwon,<sup>47</sup> J. S. Lange,<sup>4</sup> J. S. Lee,<sup>38</sup> M. J. Lee,<sup>37</sup> T. Lesiak,<sup>27</sup> A. Limosani,<sup>21</sup> S.-W. Lin,<sup>26</sup> Y. Liu,<sup>5</sup> D. Liventsev,<sup>14</sup> F. Mandl,<sup>12</sup> A. Matyjka,<sup>27</sup> S. McOnie,<sup>39</sup> T. Medvedeva,<sup>14</sup> W. Mitaroff,<sup>12</sup> K. Miyabayashi,<sup>23</sup> H. Miyata,<sup>29</sup> Y. Miyazaki,<sup>22</sup> R. Mizuk,<sup>14</sup> G. R. Moloney,<sup>21</sup> S. Nishida,<sup>9</sup> O. Nitoh,<sup>45</sup> T. Nozaki,<sup>9</sup> S. Ogawa,<sup>40</sup> T. Ohshima,<sup>22</sup> S. Okuno,<sup>16</sup> S. L. Olsen,<sup>8,11</sup> H. Ozaki,<sup>9</sup> P. Pakhlov,<sup>14</sup> C. W. Park,<sup>38</sup> L. S. Peak,<sup>39</sup> R. Pestotnik,<sup>15</sup> L. E. Piiilonen,<sup>46</sup> A. Poluektov,<sup>1</sup> H. Sahoo,<sup>8</sup> Y. Sakai,<sup>9</sup> O. Schneider,<sup>18</sup> A. J. Schwartz,<sup>3</sup> R. Seidl,<sup>10,34</sup> K. Senyo,<sup>22</sup> M. Shapkin,<sup>13</sup> V. Shebalin,<sup>1</sup> H. Shibuya,<sup>40</sup> J.-G. Shiu,<sup>26</sup> B. Shwartz,<sup>1</sup> J. B. Singh,<sup>33</sup> A. Sokolov,<sup>13</sup> A. Somov,<sup>3</sup> S. Stanič,<sup>30</sup> M. Starič,<sup>15</sup> T. Sumiyoshi,<sup>44</sup> S. Y. Suzuki,<sup>9</sup> F. Takasaki,<sup>9</sup> K. Tamai,<sup>9</sup> Y. Teramoto,<sup>31</sup> I. Tikhomirov,<sup>14</sup> S. Uehara,<sup>9</sup> K. Ueno,<sup>26</sup> T. Uglov,<sup>14</sup> Y. Unno,<sup>7</sup> S. Uno,<sup>9</sup> Y. Usov,<sup>1</sup> G. Varner,<sup>8</sup> K. Vervink,<sup>18</sup> S. Villa,<sup>18</sup> A. Vinokurova,<sup>1</sup> C. H. Wang,<sup>25</sup> P. Wang,<sup>11</sup> X. L. Wang,<sup>11</sup> Y. Watanabe,<sup>16</sup> B. D. Yabsley,<sup>39</sup> C. Z. Yuan,<sup>11</sup> Y. Yusa,<sup>46</sup> Z. P. Zhang,<sup>36</sup> V. Zhilich,<sup>1</sup> V. Zhulanov,<sup>1</sup> A. Zupanc,<sup>15</sup> and O. Zyukova<sup>1</sup>

(The Belle Collaboration)

<sup>1</sup>*Budker Institute of Nuclear Physics, Novosibirsk*

<sup>2</sup>*Chiba University, Chiba*

<sup>3</sup>*University of Cincinnati, Cincinnati, Ohio 45221*

<sup>4</sup>*Justus-Liebig-Universität Gießen, Gießen*

<sup>5</sup>*The Graduate University for Advanced Studies, Hayama*

<sup>6</sup>*Gyeongsang National University, Chinju*

<sup>7</sup>*Hanyang University, Seoul*

<sup>8</sup>*University of Hawaii, Honolulu, Hawaii 96822*

<sup>9</sup>*High Energy Accelerator Research Organization (KEK), Tsukuba*

<sup>10</sup>*University of Illinois at Urbana-Champaign, Urbana, Illinois 61801*

<sup>11</sup>*Institute of High Energy Physics, Chinese Academy of Sciences, Beijing*

<sup>12</sup>*Institute of High Energy Physics, Vienna*

<sup>13</sup>*Institute of High Energy Physics, Protvino*

<sup>14</sup>*Institute for Theoretical and Experimental Physics, Moscow*

<sup>15</sup>*J. Stefan Institute, Ljubljana*

<sup>16</sup>*Kanagawa University, Yokohama*

<sup>17</sup>*Kyungpook National University, Taegu*

<sup>18</sup>*École Polytechnique Fédérale de Lausanne (EPFL), Lausanne*

<sup>19</sup>*University of Ljubljana, Ljubljana*

<sup>20</sup>*University of Maribor, Maribor*

<sup>21</sup>*University of Melbourne, School of Physics, Victoria 3010*

<sup>22</sup>*Nagoya University, Nagoya*

<sup>23</sup>*Nara Women's University, Nara*

<sup>24</sup>*National Central University, Chung-li*

<sup>25</sup>*National United University, Miao Li*

<sup>26</sup>*Department of Physics, National Taiwan University, Taipei*

<sup>27</sup>*H. Niewodniczanski Institute of Nuclear Physics, Krakow*

<sup>28</sup>*Nippon Dental University, Niigata*

<sup>29</sup>*Niigata University, Niigata*

<sup>30</sup>*University of Nova Gorica, Nova Gorica*

<sup>31</sup>*Osaka City University, Osaka*

<sup>32</sup>*Osaka University, Osaka*

<sup>33</sup>*Panjab University, Chandigarh*

<sup>34</sup>*RIKEN BNL Research Center, Upton, New York 11973*

<sup>35</sup>*Saga University, Saga*

<sup>36</sup>*University of Science and Technology of China, Hefei*

<sup>37</sup>*Seoul National University, Seoul*<sup>38</sup>*Sungkyunkwan University, Suwon*<sup>39</sup>*University of Sydney, Sydney, New South Wales*<sup>40</sup>*Toho University, Funabashi*<sup>41</sup>*Tohoku Gakuin University, Tagajo*<sup>42</sup>*Department of Physics, University of Tokyo, Tokyo*<sup>43</sup>*Tokyo Institute of Technology, Tokyo*<sup>44</sup>*Tokyo Metropolitan University, Tokyo*<sup>45</sup>*Tokyo University of Agriculture and Technology, Tokyo*<sup>46</sup>*Virginia Polytechnic Institute and State University, Blacksburg, Virginia 24061*<sup>47</sup>*Yonsei University, Seoul*

(Received 18 October 2007; published 9 January 2008)

We report measurements of the exclusive cross section for  $e^+e^- \rightarrow D\bar{D}$ , where  $D = D^0$  or  $D^+$ , in the center-of-mass energy range from the  $D\bar{D}$  threshold to 5 GeV with initial-state radiation. The analysis is based on a data sample collected with the Belle detector with an integrated luminosity of  $673 \text{ fb}^{-1}$ .

DOI: [10.1103/PhysRevD.77.011103](https://doi.org/10.1103/PhysRevD.77.011103)

PACS numbers: 13.66.Bc, 13.87.Fh, 14.40.Gx

The total cross section for hadron production in  $e^+e^-$  annihilation in the  $\sqrt{s}$  region above the open-charm threshold was measured precisely by the Crystal Ball [1] and BES [2] Collaborations. However, the parameters of the  $J^{PC} = 1^{--}$  charmonium states obtained from fits to the inclusive cross section [3,4] are poorly understood theoretically [5]. Since interference between different resonant structures depends upon the specific final states, studies of *exclusive* cross sections for charmed meson pairs in this energy range are needed to clarify the situation. Recently, the CLEO Collaboration performed a scan over the energy range from 3.970 to 4.260 GeV and measured exclusive cross sections for  $D\bar{D}$ ,  $D\bar{D}^*$  and  $D^*\bar{D}^*$  final states at 12 points with high accuracy [6]. Belle has used a partial reconstruction technique to perform first measurements of the exclusive cross sections  $\sigma(e^+e^- \rightarrow D^\pm D^{*\mp})$  and  $\sigma(e^+e^- \rightarrow D^{*+} D^{*-})$  for  $\sqrt{s}$  near the  $D^+ D^{*-}$  and  $D^{*+} D^{*-}$  thresholds with initial-state radiation (ISR) [7]. Recently Belle [8] has reported a measurement of the exclusive cross section for the process  $e^+e^- \rightarrow D^0 D^- \pi^+$  and the first observation of  $\psi(4415) \rightarrow D\bar{D}_2^*(2460)$  decay.

In this paper we report measurements of the exclusive cross sections for the processes  $e^+e^- \rightarrow D^+ D^-$  and  $e^+e^- \rightarrow D^0 \bar{D}^0$  using ISR that are a continuation of our studies of the near-threshold exclusive open-charm production. Recently several new charmoniumlike states were observed in this mass range ( $Y(4260)$  [9,10],  $Y(4360)$ ,  $Y(4660)$  [11],  $X(4160)$  [12]) decaying to either open- or closed-charm final states. Our study provides further information on the dynamics of charm quarks at these center-of-mass energies. The data sample corresponds to an integrated luminosity of  $673 \text{ fb}^{-1}$  collected with the Belle detector [13] at the  $Y(4S)$  resonance and nearby continuum at the KEKB asymmetric-energy  $e^+e^-$  collider [14].

We select  $e^+e^- \rightarrow D\bar{D}\gamma_{\text{ISR}}$  signal events by reconstructing both the  $D$  and  $\bar{D}$  mesons, where  $D\bar{D} = D^0 \bar{D}^0$  or  $D^+ D^-$ . In general, the  $\gamma_{\text{ISR}}$  is not required to be detected; its presence in the event is inferred from a peak at

zero in the spectrum of the recoil mass against the  $D\bar{D}$  system. The square of the recoil mass is defined as

$$M_{\text{rec}}^2(D\bar{D}) = (E_{\text{c.m.}} - E_{D\bar{D}})^2 - p_{D\bar{D}}^2, \quad (1)$$

where  $E_{\text{c.m.}}$  is the initial  $e^+e^-$  center-of-mass (c.m.) energy,  $E_{D\bar{D}}$  and  $p_{D\bar{D}}$  are the c.m. energy and momentum of the  $D\bar{D}$  combination, respectively. To suppress backgrounds we consider two cases: (1) the  $\gamma_{\text{ISR}}$  is out of detector acceptance in which case the polar angle for the  $D\bar{D}$  combination in the c.m. frame is required to be  $|\cos(\theta_{D\bar{D}})| > 0.9$ ; (2) the fast  $\gamma_{\text{ISR}}$  is within the detector acceptance ( $|\cos(\theta_{D\bar{D}})| < 0.9$ ), in this case the  $\gamma_{\text{ISR}}$  is required to be detected and the mass of the  $D\bar{D}\gamma_{\text{ISR}}$  combination is required to be greater than  $E_{\text{c.m.}} - 0.58 \text{ GeV}/c^2$ . To suppress background from  $e^+e^- \rightarrow D\bar{D}(n)\pi\gamma_{\text{ISR}}$  processes we exclude events that contain additional charged tracks that are not used in the  $D$  or  $\bar{D}$  reconstruction.

We ensure that all charged tracks originate from the interaction point (IP) with the requirements  $dr < 2 \text{ cm}$  and  $|dz| < 4 \text{ cm}$ , where  $dr$  and  $|dz|$  are the impact parameters perpendicular to and along the beam direction with respect to the IP. Charged kaons are required to have a ratio of particle identification likelihoods,  $\mathcal{P}_K = \mathcal{L}_K/(\mathcal{L}_K + \mathcal{L}_\pi)$  [15], larger than 0.6. No identification requirements are applied for pion candidates.  $K_S^0$  candidates are reconstructed from  $\pi^+\pi^-$  pairs with an invariant mass within  $10 \text{ MeV}/c^2$  of the nominal  $K_S^0$  mass. The distance between the two pion tracks at the  $K_S^0$  vertex must be less than 1 cm, the transverse flight distance from the interaction point is required to be greater than 0.1 cm, and the angle between the  $K_S^0$  momentum direction and the flight direction in the  $x-y$  plane should be smaller than 0.1 rad. The pion pair candidates are refitted to the  $K_S^0$  mass. Photons are reconstructed in the electromagnetic calorimeter as showers with energies greater than 50 MeV that are not associated with charged tracks. Pairs of photons are combined to form  $\pi^0$  candidates. If the mass of a  $\gamma\gamma$  pair lies within  $15 \text{ MeV}/c^2$

of the nominal  $\pi^0$  mass, the pair is fit with a  $\pi^0$  mass constraint and considered as a  $\pi^0$  candidate.  $D^0$  candidates [16] are reconstructed using five decay modes:  $K^-\pi^+$ ,  $K^-K^+$ ,  $K^-\pi^-\pi^+\pi^+$ ,  $K_S^0\pi^+\pi^-$  and  $K^-\pi^+\pi^0$ .  $D^+$  candidates are reconstructed using the decay modes  $K_S^0\pi^+$  and  $K^-\pi^+\pi^+$ . A  $\pm 15$  MeV/ $c^2$  mass window is used for all modes except for  $K^-\pi^-\pi^+\pi^+$ , where a  $\pm 10$  MeV/ $c^2$  requirement is applied ( $\sim 2.5\sigma$  in each case). To improve the momentum resolution of  $D$  meson candidates, final tracks are fitted to a common vertex and a  $D^0$  or  $D^+$  mass constraint is applied. The  $D$  candidates from a sideband region are refitted to the mass, corresponding to the center of the sideband region with the same width as the signal window.

The distribution of  $M_{\text{rec}}^2(D\bar{D})$  after all the requirements is shown in Fig. 1(a). A clear peak corresponding to the  $e^+e^- \rightarrow D\bar{D}\gamma_{\text{ISR}}$  process is evident around zero. The shoulder at positive values is due to  $e^+e^- \rightarrow D^{(*)}\bar{D}(n)\pi^0\gamma_{\text{ISR}}$  events. To suppress the tail of such events we define a signal region by the requirement:  $|M_{\text{rec}}^2(D\bar{D})| < 0.7$  (GeV/ $c^2$ ) $^2$ . The polar angle distribution for  $D\bar{D}$  after the requirements on  $M_{\text{rec}}^2(D\bar{D})$  is shown in Fig. 1(c). The sharp peaking at  $\pm 1$  is characteristic of ISR production and agrees with the Monte Carlo (MC) simulation. The mass distribution of the  $D\bar{D}\gamma_{\text{ISR}}$  combinations where the  $\gamma_{\text{ISR}}$  is detected is shown in Fig. 1(b) after all the selection requirements. It peaks at the  $E_{\text{c.m.}}$ . The asymmetric shape of the  $M_{D\bar{D}\gamma_{\text{ISR}}}$  distribution is due to higher-order ISR processes.

The  $M_{D^0\bar{D}^0}$  and  $M_{D^+D^-}$  spectra obtained after all the requirements are shown in Fig. 2.

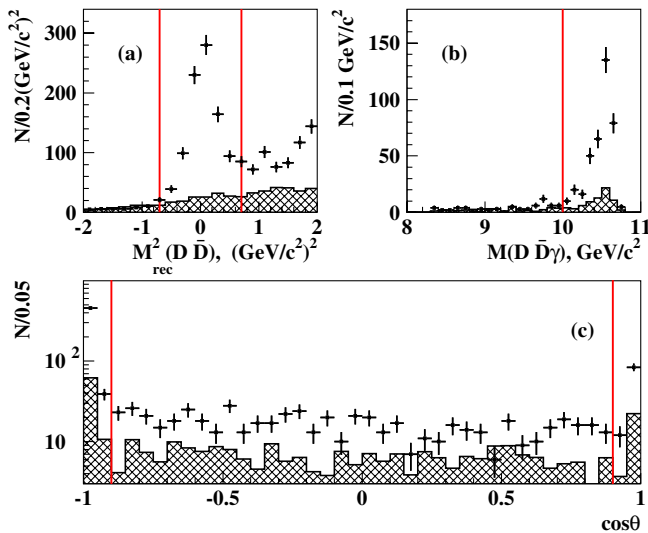


FIG. 1 (color online). The observed distributions of (a)  $M_{\text{rec}}^2(D\bar{D})$ ; (b)  $M(D\bar{D}\gamma_{\text{ISR}})$  and (c)  $D\bar{D}$  polar angles. Histograms show the normalized contributions from  $M_D$  and  $M_{\bar{D}}$  sidebands. The selected signal windows are illustrated by vertical lines.

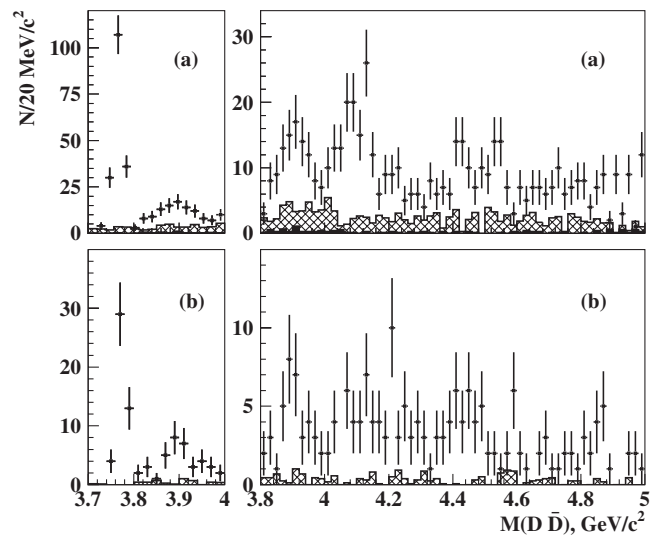


FIG. 2. The mass spectra of  $D\bar{D}$  combinations (points with error bars): (a)  $D^0\bar{D}^0$ ; (b)  $D^+D^-$ . The total contribution from combinatorial background (1–2) is shown as the hatched histogram, the contribution from background (4) is shown as the (barely visible) solid histogram.

The following sources of background are considered:

- (1) combinatorial  $D(\bar{D})$  mesons combined with a real  $\bar{D}(D)$  coming from the signal or other processes;
- (2) both  $D$  and  $\bar{D}$  are combinatorial;
- (3) reflection from the processes  $e^+e^- \rightarrow D\bar{D}\pi_{\text{miss}}^0\gamma_{\text{ISR}}$  and  $e^+e^- \rightarrow D\bar{D}\gamma_{\text{ISR}}$ , followed by  $\bar{D}^* \rightarrow \bar{D}\pi_{\text{miss}}^0$ , with an extra  $\pi_{\text{miss}}^0$  in the final state;
- (4) reflection from the process  $e^+e^- \rightarrow D\bar{D}^*\gamma_{\text{ISR}}$ , followed by  $\bar{D}^{*0} \rightarrow \bar{D}^0\gamma$ , with an extra soft  $\gamma$  in the final state;
- (5) a contribution from  $e^+e^- \rightarrow D\bar{D}\pi^0$  when an energetic  $\pi^0$  is misidentified as a single  $\gamma_{\text{ISR}}$ .

The contribution from background (1) is extracted using  $M_D$  and  $M_{\bar{D}}$  sidebands that are 4 times as large as the signal region. These sidebands are shifted by 30 MeV/ $c^2$  (20 MeV/ $c^2$  for the  $D^0 \rightarrow K^-\pi^-\pi^+\pi^+$  mode) from the signal region to avoid signal over-subtraction. Background (2) is present in both the  $M_D$  and  $M_{\bar{D}}$  sidebands and is, thus, subtracted twice. To account for this over-subtraction we use a 2-dimensional sideband region, where events are selected from both the  $M_D$  and the  $M_{\bar{D}}$  sidebands. The total contribution of the combinatorial backgrounds (1–2) is shown in Fig. 2 as a hatched histogram. Backgrounds (3–4) are suppressed by the tight requirement on  $M_{\text{rec}}^2(D\bar{D})$ . The remaining contribution from background (3) is estimated directly from the data by applying a similar full reconstruction method to the isospin-conjugate process  $e^+e^- \rightarrow D^0D^-\pi_{\text{miss}}^+\gamma_{\text{ISR}}$ . Here the requirement on absence of additional charged tracks in the event is relaxed. Since there is a charge imbalance in the  $D^0D^-$  final state, only events with an extra missing  $\pi_{\text{miss}}^+$  can contribute to the  $M_{\text{rec}}^2(D\bar{D})$  signal window. To extract the level of back-

ground (3), the  $D^0 D^-$  mass spectrum is rescaled according to the ratio of  $D^0$  and  $D^-$  reconstruction efficiencies and an isospin factor of 1/2. When this is done, the contribution from background (3) is found to be negligibly small. Uncertainties in this estimate are included in the systematic error. Background (4) contributes only to the  $D^0 \bar{D}^0$  final state. It is estimated using an MC simulation of  $e^+ e^- \rightarrow D^0 \bar{D}^{*0} \gamma_{\text{ISR}}$ , followed by  $\bar{D}^{*0} \rightarrow \bar{D}^0 \gamma$ . To reproduce the shape of the  $D^0 \bar{D}^{*0}$  mass distribution we use the  $D^\pm D^{*\mp}$  cross section measured in our previous study [7]. The contribution from background (4) is found to be small (shown in Fig. 2(a) as a solid histogram) and is subtracted from the  $D^0 \bar{D}^0$  mass spectrum. Uncertainties in this estimate are included in the systematic error. The contribution from background (5), determined from reconstructed  $e^+ e^- \rightarrow D \bar{D} \pi^0$  events in the data, is found to be negligibly small and taken into account in the systematic error.

The  $e^+ e^- \rightarrow D \bar{D}$  cross sections are extracted from the  $D^0 \bar{D}^0$  and  $D^+ D^-$  mass distributions [17]

$$\sigma(e^+ e^- \rightarrow D \bar{D}) = \frac{dN/dm}{\eta_{\text{tot}} dL/dm}, \quad (2)$$

where  $m \equiv M_{D\bar{D}}$ ,  $dN/dm$  is the obtained mass spectra, while  $\eta_{\text{tot}}$  is the total efficiency. The factor  $dL/dm$  is the differential ISR luminosity

$$dL/dm = \frac{\alpha}{\pi x} \left( (2 - 2x + x^2) \ln \frac{1+C}{1-C} - x^2 C \right) \frac{2m \mathcal{L}}{E_{\text{c.m.}}^2}, \quad (3)$$

where  $x = 1 - m^2/E_{\text{c.m.}}^2$ ,  $\mathcal{L}$  is the total integrated luminosity and  $C = \cos\theta_0$ , where  $\theta_0$  defines the polar angle range for the  $\gamma_{\text{ISR}}$  in the  $e^+ e^-$  c.m. frame:  $\theta_0 < \theta_{\gamma_{\text{ISR}}} < 180^\circ - \theta_0$ . The total efficiency determined by MC simulation grows linearly with  $M_{D\bar{D}}$  from 0.095% near threshold to 0.46% at 5 GeV/ $c^2$  for the  $D^0 \bar{D}^0$  and from 0.038% to 0.17% for the  $D^+ D^-$  mode. The resulting  $e^+ e^- \rightarrow D^0 \bar{D}^0$ ,  $e^+ e^- \rightarrow D^+ D^-$  and  $e^+ e^- \rightarrow D \bar{D}$  exclusive cross sections, averaged over the bin width, are shown in Fig. 3 with statistical uncertainties only.

Since the bin width in the cross section distributions is much larger than the resolution (which is  $\sim 3$  MeV/ $c^2$  at threshold and  $\sim 5$  MeV/ $c^2$  at  $M_{D\bar{D}} \sim 5$  GeV/ $c^2$ ), no correction for resolution is applied.

We calculate the cross section ratio  $\sigma(e^+ e^- \rightarrow D^+ D^-)/\sigma(e^+ e^- \rightarrow D^0 \bar{D}^0)$  for the  $M_{D\bar{D}}$  bin (3.76–3.78) GeV/ $c^2$  corresponding to  $M_{D\bar{D}} \approx M_{\psi(3770)}$  to be  $(0.72 \pm 0.16 \pm 0.06)$ . This value is in agreement within errors with the CLEO Collaboration [18] and BES [19] measurements. The ratio  $\sigma(e^+ e^- \rightarrow D^+ D^-)/\sigma(e^+ e^- \rightarrow D^0 \bar{D}^0)$  integrated over the  $M_{D\bar{D}}$  range from 3.8 to 5.8 GeV/ $c^2$  is found to be  $(1.15 \pm 0.13 \pm 0.10)$  and is consistent with unity.

The systematic errors for the  $\sigma(e^+ e^- \rightarrow D \bar{D})$  measurements are summarized in Table I.

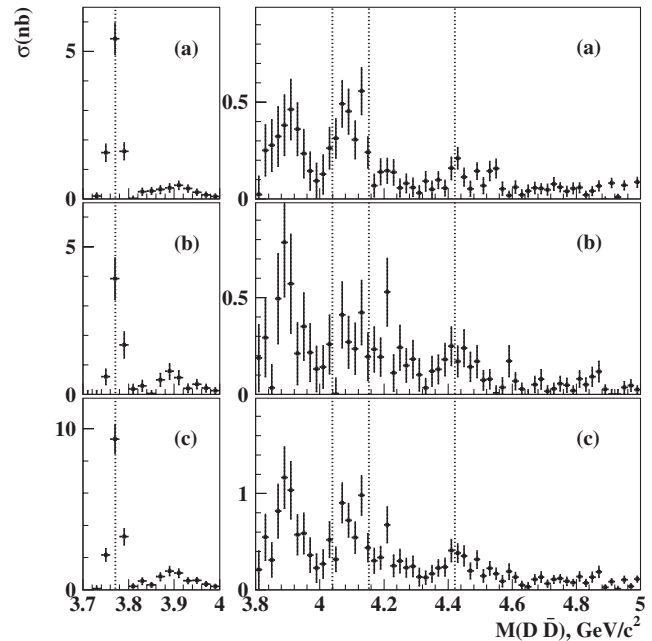


FIG. 3. The exclusive cross sections for (a)  $e^+ e^- \rightarrow D^0 \bar{D}^0$ ; (b)  $e^+ e^- \rightarrow D^+ D^-$ ; (c)  $e^+ e^- \rightarrow D \bar{D}$ . The dotted lines correspond to the  $\psi(3770)$ ,  $\psi(4040)$ ,  $\psi(4160)$  and  $\psi(4415)$  masses [20].

The systematic errors associated with the background (1–2) subtraction are estimated to be 2% due to the uncertainty in the scaling factors for the sideband subtractions. This systematic error is estimated using fits to the  $M_D$  and  $M_{\bar{D}}$  distributions with different signal and background parametrizations. Uncertainties in backgrounds (3–5) are conservatively estimated to be smaller than 2% of the signal in the case of  $D^0 \bar{D}^0$ ; these two sources are added linearly to give 4% in total. In the  $D^+ D^-$  case, backgrounds (3–5) are estimated using the data and only the uncertainty in the scaling factor for the subtracted distributions is taken into account. A second source of systematic error comes from the uncertainties in track and photon reconstruction efficiencies, which are 1% per track, 1.5% per photon and 5% per  $K_S^0$ , respectively. The systematic error ascribed to the cross section calculation is estimated to be 5% and includes the error on the differential ISR luminosity and the error from the efficiency fit. Other contributions come from the uncertainty in the identifica-

TABLE I. Contributions to the systematic error in the cross sections, [%].

Source	$D^0 \bar{D}^0$	$D^+ D^-$	$D \bar{D}$
Background subtraction	$\pm 4$	$\pm 3$	$\pm 3$
Reconstruction	$\pm 7$	$\pm 6$	$\pm 7$
Cross section calculation	$\pm 5$	$\pm 5$	$\pm 5$
$\mathcal{B}(D)$	$\pm 4$	$\pm 6$	$\pm 5$
Kaon identification	$\pm 2$	$\pm 2$	$\pm 2$
Total	$\pm 10$	$\pm 10$	$\pm 10$

tion efficiency and the absolute  $D^0$  and  $D^+$  branching fractions [20]. The total systematic uncertainties are 10% and comparable to the statistical errors in the differential cross section around the  $\psi(3770)$  peak; for the other  $M_{D\bar{D}}$  ranges statistical errors dominate.

In summary, we report measurements of  $e^+e^- \rightarrow D^0\bar{D}^0$  and  $e^+e^- \rightarrow D^+D^-$  exclusive cross sections for  $\sqrt{s}$  near the  $D^0\bar{D}^0$  and  $D^+D^-$  thresholds with initial-state radiation. The observed  $e^+e^- \rightarrow D\bar{D}$  exclusive cross sections are consistent with recent *BABAR* measurements [21] and are in qualitative agreement with the coupled-channel model predictions of Ref. [22]. This includes the peak at 3.9 GeV/ $c^2$  that is seen both in Belle and *BABAR* cross section spectra.

We thank the KEKB group for the excellent operation of the accelerator, the KEK cryogenics group for the efficient operation of the solenoid, and the KEK computer group and the National Institute of Informatics for valuable computing and Super-SINET network support. We acknowledge support from the Ministry of Education, Culture,

Sports, Science, and Technology of Japan and the Japan Society for the Promotion of Science; the Australian Research Council and the Australian Department of Education, Science and Training; the National Science Foundation of China and the Knowledge Innovation Program of the Chinese Academy of Sciences under Contract No. 10575109 and IHEP-U-503; the Department of Science and Technology of India; the BK21 program of the Ministry of Education of Korea, the CHEP SRC program and Basic Research program (Grant No. R01-2005-000-10089-0) of the Korea Science and Engineering Foundation, and the Pure Basic Research Group program of the Korea Research Foundation; the Polish State Committee for Scientific Research; the Ministry of Education and Science of the Russian Federation and the Russian Federal Agency for Atomic Energy; the Slovenian Research Agency; the Swiss National Science Foundation; the National Science Council and the Ministry of Education of Taiwan; and the U.S. Department of Energy.

- 
- [1] A. Osterheld *et al.* (Crystal Ball Collaboration), SLAC-PUB-4160, 1986.
- [2] J. Z. Bai *et al.* (BES Collaboration), Phys. Rev. Lett. **88**, 101802 (2002).
- [3] K. K. Seth, Phys. Rev. D **72**, 017501 (2005).
- [4] M. Ablikim *et al.* (BES Collaboration), arXiv:0705.4500.
- [5] T. Barnes, S. Godfrey, and E. S. Swanson, Phys. Rev. D **72**, 054026 (2005).
- [6] R. Poling (for CLEO Collaboration), arXiv:0606016.
- [7] G. Pakhlova *et al.* (Belle Collaboration), Phys. Rev. Lett. **98**, 092001 (2007).
- [8] G. Pakhlova *et al.* (Belle Collaboration), arXiv:0708.3313 [Phys. Rev. Lett. (to be published)].
- [9] B. Aubert *et al.* (*BABAR* Collaboration), Phys. Rev. Lett. **95**, 142001 (2005).
- [10] C. Z. Yuan *et al.* (Belle Collaboration), Phys. Rev. Lett. **99**, 182004 (2007).
- [11] X. L. Wang *et al.* (Belle Collaboration), Phys. Rev. Lett. **99**, 142002 (2007).
- [12] K. Abe *et al.* (Belle Collaboration), arXiv:0708.3812 [Phys. Rev. Lett. (to be published)].
- [13] A. Abashian *et al.* (Belle Collaboration), Nucl. Instrum. Methods Phys. Res., Sect. A **479**, 117 (2002).
- [14] S. Kurokawa and E. Kikutani, Nucl. Instrum. Methods Phys. Res., Sect. A **499**, 1 (2003); and other papers included in this volume.
- [15] E. Nakano, Nucl. Instrum. Methods Phys. Res., Sect. A **494**, 402 (2002).
- [16] Charge-conjugate modes are included throughout this paper.
- [17] E. A. Kuraev and V. S. Fadin, Sov. J. Nucl. Phys. **41**, 466 (1985) [Yad. Fiz. **41**, 733 (1985)].
- [18] S. Dobbs *et al.* (CLEO Collaboration), Phys. Rev. D **76**, 112001 (2007).
- [19] M. Ablikim *et al.* (BES Collaboration), Phys. Lett. B **630**, 14 (2005).
- [20] W.-M. Yao *et al.* (Particle Data Group), J. Phys. G **33**, 1 (2006).
- [21] B. Aubert *et al.* (*BABAR* Collaboration), Phys. Rev. D **76**, 111105 (2007).
- [22] E. Eichten, K. Gottfried, T. Kinoshita, K. D. Lane, and Tung-Mow Yan, Phys. Rev. D **21**, 203 (1980).